



SMART-X, “Square Meter, Arcsecond Resolution Telescope for X-rays”

A. Vikhlinin^{1,2}

¹ On behalf of the *SMART-X* collaboration, see <http://hea-www.cfa.harvard.edu/SMARTX/>

² Harvard-Smithsonian Center for Astrophysics e-mail: avikhlinin@cfa.harvard.edu

Abstract. *SMART-X* is a mission concept for a 2.3 m² effective area, 0.5'' angular resolution X-ray telescope, with 5' FOV, 1'' pixel size microcalorimeter, 22' FOV imager, and high-throughput gratings.

1. Introduction

We describe the Square Meter Arcsecond Resolution X-ray Telescope — *SMART-X*. This concept leverages an emerging adjustable optics technology to build a mission more scientifically ambitious than the International X-ray Observatory, but more efficiently. Our *SMART-X* concept includes substantial simplifications and cost reductions relative to *IXO* — shorter focal length eliminating the extendable optical bench and reducing mass and structural complexity, fewer science instruments, and streamlined operations — and in this, it is similar to many modifications to the *IXO* studied in the last two years. Adding subarcsecond resolution, *SMART-X* will build upon *Chandra*'s success and *IXO*'s ambitions, becoming a major and indisputable scientific advance at an affordable cost. To generate sustained support, a mission concept should be able to capture the imagination of the scientific community, and *SMART-X* will do exactly that.

SMART-X will be capable of addressing almost all of the *IXO* science goals — growth of SMBH and strong gravity effects; evolution of large scale structure and detection of

the WHIM; AGN feedback and cycles of matter and energy. In many areas, *SMART-X* transcends the scope of *IXO*. It will be able to carry out surveys to the *Chandra* deep fields depth over 10 deg²; study galaxy assembly processes to $z = 2.5$; and track the evolution of group-sized objects, including those hosting the first quasars, to $z = 6$; open new opportunities in the time domain and high-resolution spectroscopy.

Over the past few years we have developed the concept of the adjustable-optic telescope. With some initial technical success, we now believe that it is timely to introduce this approach to the discussion of future directions in X-ray astronomy. The challenge is to develop the optics to a high level of technical readiness over the next several years to provide *Chandra*-like 0.5'' half-power diameter angular resolution with *IXO*-like area (2.3 m² at 1 keV or ≈ 30 times *Chandra*). This is a tremendous increase — recall that a factor of 4 increase in area from Palomar to Keck was considered a breakthrough at the time. With Keck, there were additional scientific gains from detector advances. For *SMART-X*, we also plan for advanced instruments: 1) an active pixel sensing imager for surveys, sub-arcsecond imag-

ing, and soft-band response; 2) a $5' \times 5'$ field of view microcalorimeter with $1''$ pixels and 5 eV energy resolution; and 3) a high throughput X-ray grating spectrometer.

The baseline plan for *SMART-X* optics uses slumped glass mirror segments with deposited piezoelectric actuators energized to correct mirror figure errors from $10''$ (achieved for IXO) to $\lesssim 0.5''$. This concept builds upon the mirror development for IXO, both in terms of the thermally formed substrates, as well as mirror alignment and mounting. Work on the optics technology is already underway, with both the baseline option and several alternatives being actively studied.

With funding for mission studies and technology in a few key areas during the current decade, *SMART-X* can be developed and launched in the 2020's. Whether or not ATHENA or AXSIO proceeds in this decade, *SMART-X* is a qualitative leap forward and is the logical candidate for *the* major X-ray mission of the 2020's.

2. SMART-X optics

The *SMART-X* mirror design draws from previous IXO studies and uses slumped glass segments. The 3 m diameter aperture is covered with 292 shells forming a Wolter-type¹ mirror with a 10m focal length. Mirror segments are 200mm long with azimuthal spans ranging from 150 to 380mm. This model has been ray-traced assuming an Ir coating and accounting for structural obscurations, large angle scattering, contamination, and small alignment errors. Raytrace calculation gives an effective area (EA) of 2.3 m^2 at 1 keV (see Fig. 2 below) and shows that the blur due to off-axis aberrations from the Wolter-I design is within $0.5''$ half power diameter out to $2.5'$ off-axis. Losses in effective area due to shadowing and vignetting are less than 50% for all energies out to $\sim 8.5'$ off-axis. At 2 keV, loss of EA is

¹ Our present estimated are based on ray-trace modeling of a Wolter-I telescope; we will also consider a Wolter-Schwarzschild and polynomial designs to improve the off-axis point response function.

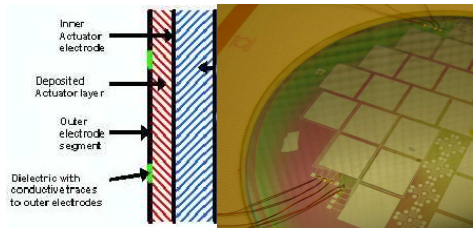


Fig. 1. Left: Cross-sectional schematic of the PZT cell structure. Right: A photo of a flat Corning Eagle™ test mirror with deposited PZT film and a pattern of the independently addressable electrodes.

$< 20\%$ within the inner $10'$, providing a useful field of view of at least $20' \times 20'$ for survey work and imaging of extended sources.

The mirror segments are made of either $400 \mu\text{m}$ thick thermally formed glass sheets (similar to those used in LCD displays), or $100\text{--}200 \mu\text{m}$ thick electroformed nickel/cobalt replicated mirror segments. The flight mirror assembly mass is estimated at 890 kg, where the mirror segments and support structure each contribute 50%.

Our approach to achieving $0.5''$ angular resolution with segmented, lightweight mirrors is to make each individual segment adjustable. A ground electrode is deposited on the back of the mirror, then a thin ($1\text{--}5 \mu\text{m}$) layer of piezoelectric material (lead zirconate titanate, or PZT) is deposited on the ground electrode; and lastly, a “pixelated” array of independently addressable electrodes is deposited on the piezo material to form an array of piezo “cells”. As a voltage is applied between the ground electrode and one of the back surface electrodes, strain in the piezo cell causes controllable local bending in the mirror. By controlling the voltage applied to each cell, the correction can be made to match the local figure errors in the mirror, correcting the thin mirror figure to a level not achievable by ordinary means. The appropriate voltage is applied to each cell for the duration of the mission. Nominal leakage current is only $\sim 0.01 \text{ mA}$ at 10 V, so operating power even for 10^6 adjusters is a few hundred watts.

We project that a mirror figure quality corresponding to $0.5''$ angular resolution can be achieved by having the individual segments

adjusted essentially once. Figure errors after mounting and alignment will be measured by optical surface metrology. These errors as well as deformations due to gravity release and the nominal on-orbit thermal environment will be corrected by applying an optimal set of voltages to each mirror segment. Depending on mission safety requirements, the piezos can either be left energized through launch, or the power supplies turned off, and the piezos energized once on-orbit.

SAO and PSU working together have made significant progress with adjustable X-ray optics, and we consider the technology to be at TRL2 and approaching 3². Thin films of piezoelectric material was successfully deposited on flat test mirrors (Fig. 1), and the energizing of that piezo to produce a localized figure change consistent with expectations. Piezo thickness, properties, and achieved strain (800 ppm) meet requirements dictated by starting with an $\sim 10''$ PSF for an uncorrected mirror pair and correcting it to $< 0.5''$.

For latest information on the current state and development plans for the adjustable X-ray optics technology, visit <http://hea-www.cfa.harvard.edu/SMARTX>. Here we note, that the technology can be brought to a NASA “readiness level 6” by 2019. We are also on track to achieve within the next 3 years an adjustable mirror pair whose performance, consistent with subarcsec imaging, will be verified in an X-ray test.

We envision three science instruments for *SMART-X*. The deployable Critical Angle Transmission Grating Spectrometer (CATGS) will provide a resolving power of $R > 4000$ with large collecting area across the 0.2–1.2 keV energy band. The two prime focus imaging instruments, on a movable translation stage, are complementary and provide some redundancy. The Active Pixel Sensor Imager (APSI) is optimized for high-resolution imaging, provides a large FOV ($22' \times 22'$) for surveys, and has excellent response at $E < 0.5$ keV for studies of high-redshift ob-

² Note also that a subset of this technology is already being used for 1-D correction of synchrotron X-ray optics (Alcock 2011).

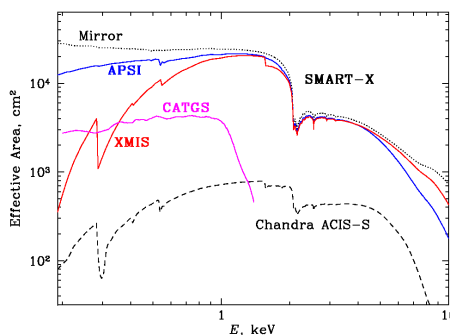


Fig. 2. Effective area of the *SMART-X* optics and science instruments.

jects. The X-ray Microcalorimeter Imaging Spectrometer (XMIS) provides 5 eV spectroscopy and good high- E efficiency, while still maintaining $1''$ imaging. The zeroth-order image in the prime focus can be taken using either APSI or XMIS.

3. SMART-X science

Except for sensitivity at $E > 10$ keV and timing for 10^6 cnt s^{-1} , *SMART-X* meets or exceeds all requirements for achieving the core science goals of the *IXO*. The high angular resolution emphasized in the *SMART-X* design enables science well beyond that considered by Astro2010 for *IXO*. It will open new windows for X-ray astronomy in studies of the high- z Universe, in the time domain, and in high-resolution spectroscopy. In the space remaining, we give only two examples of what *SMART-X* would achieve.

3.1. Supermassive black holes and their environment to $z = 6$ and beyond.

Studies of the first generation of black holes and their host galaxies which by $z \approx 6$ have ionized nearly all of the hydrogen in the Universe is one of the major topics highlighted by Astro2010.

Quasars at $z \sim 6$, discovered in the SDSS and other surveys (Fan et al. 2006; Willott et al. 2010; Mortlock et al. 2011), are extremely lu-

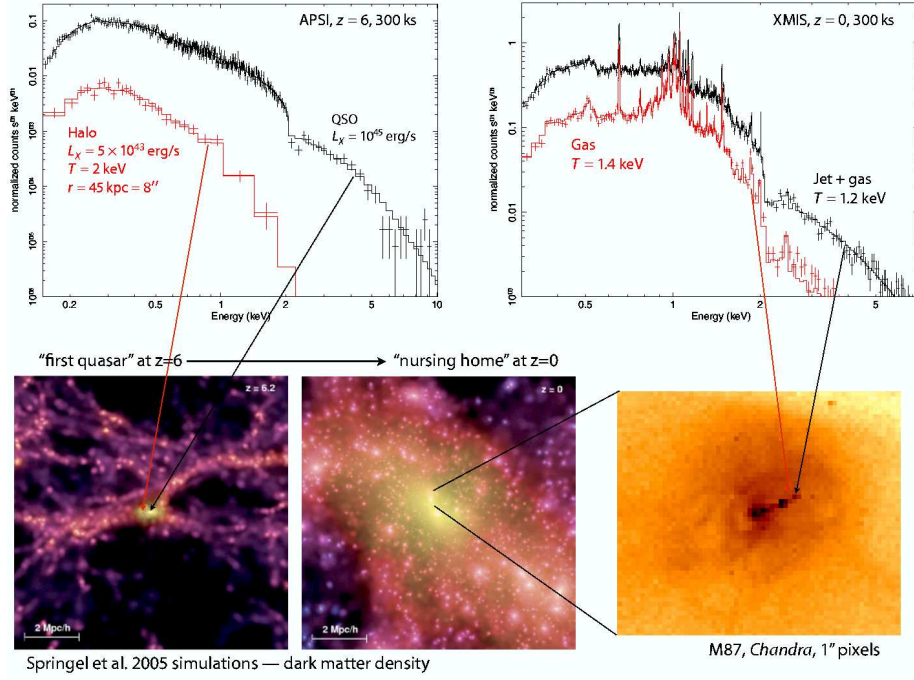


Fig. 3. SMART-X view of the environment of the “first quasars” and their descendants at $z = 0$. Sloan quasars must be located in the most massive halos existing at $z = 6$, $M = (2-6) \times 10^{12} M_{\odot}$ with $r_{\text{vir}} \approx 50$ kpc (Springel et al. 2005). These halos resemble cores of today’s rich galaxy clusters both in terms of the dark matter density and X-ray properties [$T = 1.5 - 3$ keV, $L_X = (2 - 9) \times 10^{43}$ erg s^{-1}]. SMART-X will be able to separate this faint halo from the bright quasar emission *spatially* in a 300 ksec APSI observation. Descendants of the first quasars at $z = 0$ are at the centers of rich galaxy clusters. A 300 ksec observation of a low- z cluster core with XMIS yields enough counts for detailed spectroscopy in $1'' \times 1''$ regions.

minous and massive, $M_{\text{BH}} \sim 10^9 M_{\odot}$ (Willott et al. 2010). To form such a massive BH at high z is a great challenge for theory. Depending on the typical accretion rate, the progenitor masses at $z = 10$ range from $M_{\text{BH}} \sim 3 \times 10^8 M_{\odot}$ for $\dot{M} = 0.1 \dot{M}_{\text{Edd}}$ to $\sim 7500 M_{\odot}$ for an Eddington rate. Observations of this progenitor population are one of the best ways to solve the puzzle of the seed BH origin (Volonteri 2010).

Many $z = 6$ quasars are detected in short *Chandra* observations to have $L_X \sim 10^{45}$ erg s^{-1} (Shemmer et al. 2006). Assuming that $L_X \propto M_{\text{BH}}$, we expect $L_X \approx 3 \times 10^{44}$ erg s^{-1} for a $3 \times 10^8 M_{\odot}$ SMBH at $z = 10$. SMART-X sensitivity is sufficient for spectroscopy of such quasars, even if they are highly obscured and thus undetectable in the optical or IR. In a medium-sensitivity survey observation,

100 ksec with APSI, a 10 photons detection threshold at $z = 10$ corresponds to a low-luminosity AGN, $L_X = 6.5 \times 10^{42}$ erg s^{-1} or $M_{\text{BH}} \approx 6.5 \times 10^6 M_{\odot}$. SMART-X will be able to survey ~ 10 deg 2 to this depth, so any significant population of such SMBH at $z = 10$ will be uncovered.

The growth of SMBH is intimately connected with the properties and environment of their host galaxies. SMART-X will be able to directly study the connection to $z = 6$. Springel et al. (2005) argue that the $M_{\text{BH}} \sim 10^9 M_{\odot}$ Sloan quasars must be located in the biggest galaxies and hence in the biggest dark matter halos existing at that epoch. These host halos resemble the cores of today’s galaxy clusters both in their X-ray properties and dark matter density, $M_{\text{tot}} = (2 - 6) \times 10^{12} h^{-1} M_{\odot}$,

$r_{\text{vir}} \approx 50$ kpc, $T = 1.5 - 3$ keV and $L_X = (2 - 9) \times 10^{43}$ erg s $^{-1}$. Although the halo X-ray emission is only a small fraction of the quasar's flux, and normally is undetectable, *SMART-X*, can easily separate the quasar and the halo *spatially* ($1'' = 5.5$ kpc at $z = 6$), and in a 300 ksec APSI observation the halo's gas temperature will be measured (Fig. 3).

Through detailed *SMART-X* spectroscopy of quasars at $z \leq 6$, we can detect powerful SMBH-driven winds (Chartas et al. 2009), use Fe line to detect the presence of multiple SMBHs (Li et al. 2007), and in some cases observe strong gravity effects.

Fast-forwarding to $z = 0$, the SMBHs of the first quasars should lie at the centers of rich galaxy clusters (Springel et al. 2005), and many have switched to "radio-mode" (e.g., Merloni & Heinz 2008). A moderately-deep XMIS observation (300 ksec) of a low- z cluster will provide an amazingly detailed picture of the "nursing home of the first quasar"; enough photons for detailed spectroscopy will be collected in individual $1'' \times 1''$ pixels (Fig. 3, right). Even at $z = 0.5$, *SMART-X* will be able to observe interactions of AGNs with the cluster gas with a remarkable level of detail.

3.2. Surveys.

SMART-X can carry out surveys matching the scope of the future deep optical, IR, and mm/submm surveys. Its instrumental background is close to *Chandra*'s because of the same focal length and similar orbit, $\approx 10^{-6}$ cnt arcsec $^{-2}$ s $^{-1}$. If we consider detections in the 0.7–2 keV band where the Galactic foreground contamination is low (Markevitch et al. 2003), then for typical power law spectra, *SMART-X*/APSI has a factor of ~ 50 higher throughput than *Chandra*/ACIS-I — a combined gain of factors of 30 and 1.6 due to the mirror area and soft-band QE of APSI, respectively. Therefore, the sensitivity limit of the 4 Msec *Chandra* Deep Field South will be reached with *SMART-X* in 80 ksec. Sensitivity will be fully photon-limited because even at $10'$ off-axis where the PSF is $4''$ HPD, there will be only 1 background event per resolution element at this exposure. The *Chandra* PSF de-

grades to $4''$ HPD at $7'$ off-axis, so *SMART-X* provides not only a higher sensitivity but also a wider FOV. The grasp of *SMART-X* is a factor of 98 higher than *Chandra*'s. A 10 deg^2 survey to the CDFS depth can be carried out in 8.1 Msec. A 4 Msec individual pointing will reach on-axis sensitivity (for 10 cnt detections) of 3.0×10^{-19} erg s $^{-1}$ cm $^{-2}$ in the 0.5–2 keV band, corresponding to $L_X^{(2-10)} = 3.3 \times 10^{41}$ erg s $^{-1}$ at $z = 10$.

4. SMART-X mission

We envision the launch of *SMART-X* to a 700,000 km orbit about the L2 point. The total mass of the *SMART-X* payload is 2863 kg (this includes an estimated mass, 1300 kg, of the spacecraft with the optical bench). With a 30% growth contingency and 200 kg propellant, the total "wet" mass is 3922 kg. This is comfortably launchable with Atlas V-541 (> 5000 kg throw mass).

The mission design and operations share great similarities to both *Chandra* and AXSIO. Compared to *Chandra*, *SMART-X* has a slightly lower (17%) overall mass, while the telescope assembly mass is 28% less. Key requirements — including alignment, stability, pointing control and aspect determination — will be essentially the same, and therefore require no new technology. The main difference is higher peak science data rates, and increased power requirements for thermal control of the optics and operating XMIS. Compared to AXSIO, *SMART-X* will share the same general layout, but with an updated optic, a second focal plane instrument, and a translation stage, resulting in $\approx 30\%$ larger mass and power requirements. Much of the *Chandra* ground software for all aspects of operations and science can be reused for *SMART-X*.

4.1. Cost.

The major new technology development required to realize the *SMART-X* mission is the adjustable optics to provide the large area, low mass, $0.5''$ resolution telescope at an affordable price. The cost of this program is estimated at \$45M in the next 6–8 yr — a rather

modest investment to achieve the gains possible with *SMART-X*. An additional technology investment of ~\$30M is required to bring the science instruments to TRL 5/6. Even though the *SMART-X* concept is new and has not been evaluated by the MDL, much of the work done for AXSIO is directly relevant, as is the *Chandra* experience. We can start with the detailed assessment done by the AXSIO team and the MDL and then identify differences for *SMART-X*. Using this approach, we estimate the total end-to-end mission cost of ~2.3B for *SMART-X* (see Vikhlinin et al. 2011, for details).

We can independently cross-check this cost estimate against the actual cost of building *Chandra*, \$2,521M in FY2012 dollars. This should be compared against the estimated cost of *SMART-X* excluding launch, ground system, and post-launch operations — \$1,838M, obtained by adding *SMART-X* extras to the corresponding cost of AXSIO. The inflated *Chandra* cost is most certainly an overestimate because it is based on labor rates while parts and components have escalated less. Also, technology investments already made as well as the *Chandra* knowledge base and experience are significant savings factors for *SMART-X* (e.g., optics metrology is in hand for *SMART-X* but had to be developed for *Chandra*).

The *SMART-X* mission concept for a 2.3 m², 0.5'' resolution X-ray telescope, with 5' FOV, 1'' pixel size microcalorimeter, 22' FOV imager, and high-throughput gratings, is challenging. However, we will be working with known requirements and capabilities, once the mirror technology is proven. The science will be extraordinary.

References

- Alcock, S., 2011, 4th Workshop on Adaption and Active X-ray and XUV Optics <http://www.diamond.ac.uk/Home/actop/programme.html>
- Chartas, G., et al., 2009, ApJ, 706, 644
- Fan, X., et al. 2006, ApJ, 132, 117
- Li, Y., et al. 2007, ApJ, 665, 187
- Markevitch, M., et al. 2003, ApJ, 583, 70
- Merloni, A. & Heinz, S. 2008, MNRAS, 388, 1011
- Mortlock, D. J., et al. 2011, Nature, 474, 616
- Shemmer, O., et al. 2006, ApJ, 644, 86
- Springel, V., et al. 2005, Nature, 435, 629, millenium simulation
- Vikhlinin, A. et al. 2011, <http://hea-www.cfa.harvard.edu/SMARTX/presentations/smx-rfi-submitted.pdf>
- Volonteri, M. 2010, A&A Rev., 18, 279
- Willott, C. J., et al. 2010, ApJ, 140, 546